EFFICIENT PHOSPHORESCENT OLEDS BASED ON VACUUM DEPOSITION TECHNOLOGY

Desta Gebeyehu
Department of Physics
Addis Ababa University

and

K. Leo
Institute of Applied Photophysics (IAPP)
Technology University of Dresden, Germany

ABSTRACT

Organic light emitting devices (OLEDs) are viewed as a potential next generation display and lighting applications. Phosphorescent OLED technology, with its inherently high efficiencies, represents the best opportunity to meet the challenging requirements of display and lighting applications. Thereby, we demonstrate high-efficiency organic light-emitting diodes by incorporating a double emission layer {i.e. both doped with the green phosphorescent dye tris(phenylpyridine)iridium [Ir(ppy)$_3$]} into p-i-n-type device structure based on vacuum deposition technology. The intrinsic and doped transports layers are formed using a high vacuum controlled co-evaporation deposition technique. These have been very successful in reducing the operational voltages and increasing the power efficiency. A peak power efficiency of 77 lm/W and an external quantum efficiency of 19 % are achieved at 100 cd/m^2 and at an operating voltage of 2.65 V.

Keywords: p-i-n structure, Phosphorescent OLED, Double doped emission layers.

INTRODUCTION

Organic light emitting diodes are currently under intense investigation for use in the next generation of display and lighting applications. The benefits of these technologies include wide viewing angle, color-tunable, planar light sources, fast response times, high emission efficiencies that result in high brightness with low power consumption and low operating voltage over conventional silicon devices. As OLED devices are very lightweight they may be used in cellular phones, notebooks, digital video cameras, digital versatile disc (DVD) players, car stereos, televisions and many other consumer tools that require colour displays.

The operation principle of organic light emitting diodes comprises four consecutive fundamental steps as shown in Fig. 1(a) below: (1) opposite sign charge carrier injection, (2) charge carriers transport, (3) generation of excitons, and (4) radiative exciton decay leading to emission of light. The basic OLED cell structure consists of a stack of thin organic layers sandwiched between a transparent anode and a metallic cathode. The anode injects holes into the first organic layer referred as the "hole injection layer", while the cathode injects electrons into its adjacent layer. In addition to the hole injection layer the basic OLED cell structure also compromises a "hole transport layer", an "emissive layer" and an "electron transport layer". When an appropriate voltage (typically a few volts) is applied to the cell the injected positive and negative charges recombine in the emissive layer to produce light (electroluminescence). The structure of the organic layers and the choice of the anode and cathode are designed to maximise the recombination process in the emissive layer, thus maximising the light output from the OLED device (see Fig. 1(b)).
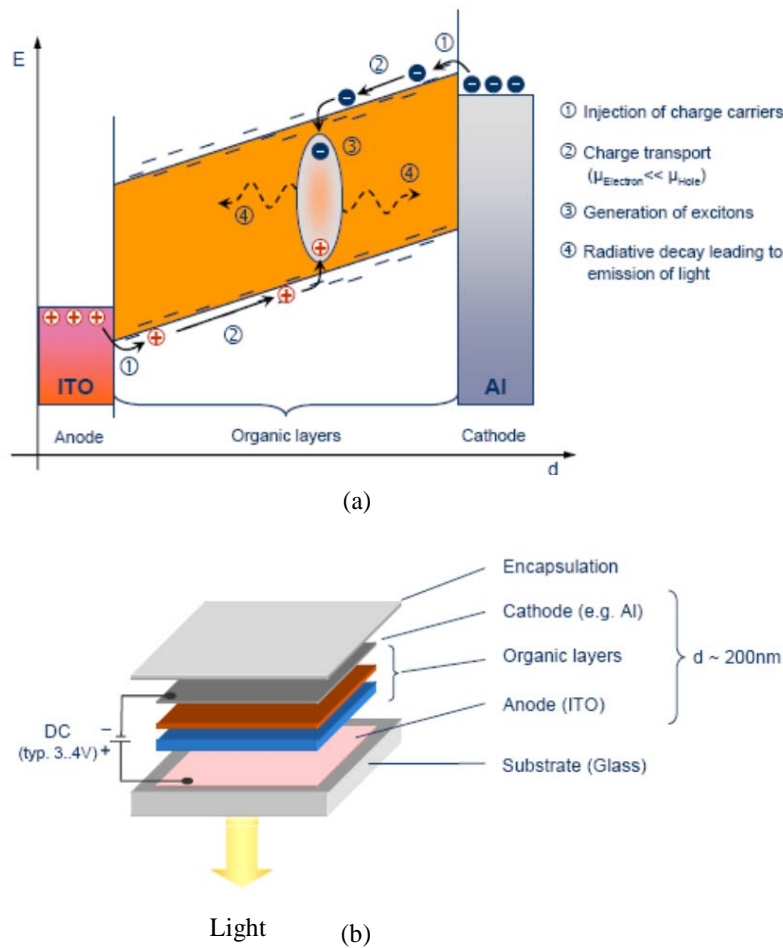
(a)

(b)

Figure 1   (a) OLED working principle and (b) thin-film layers of organic materials sandwiched between anode and cathode

Light-emitting materials for these devices can be divided into two general classes, those that are fluorescent and those that are phosphorescent. Phosphorescent systems are the focus of much recent development, because, in spite of their relative long-lived emissive state they are able to fully utilize all the charge injected for emission. In contrast in fluorescent systems, triplet formation leads to a substantial loss of efficiency. Furthermore, organic light-emitting devices using phosphorescent dyes doped into charge transporting hosts as emissive layer have attracted intensive attention [1-4] due to the ability of highly efficient emission compared with conventional fluorescent OLEDs. Through radiative recombination of singlet and triplet excitons, the internal quantum efficiency of the phosphorescent OLEDs can reach 100% [5-7] corresponding to an external quantum efficiency of around 20% limited by the light outcoupling factor. Adachi et al.[7] reported a maximum external quantum efficiency of 15.4% by doping a green-emitting phosphorescent dye, tris(phenylpyridine)iridium [Ir(ppy)$_3$], into an electron transporting host, 3-phenyl-4-(1'-naphthyl)-5-phenyl-1,2,4-triazole (TAZ). Ikai et al.[6] employed perfluorinated starburst phenylenes as a both hole- and exciton-blocking layer and a hole transport material 4,4',4"-tris(N-carbazolyl)-triphenylamine (TCTA) as a host for Ir(ppy)$_3$ and obtained an external quantum efficiency of 19.2%. However, most of these high efficiency phosphorescent OLEDs work at comparatively high voltage, and the high efficiency is mostly obtained at very low current density and brightness, and then decrease rapidly with increasing current. This is a big challenge for applications such as very high brightness displays, passive matrix driven displays or OLEDs for lighting applications. Unfortunately, it is generally difficult to obtain high quantum efficiency at high current densities due to triplet-triplet annihilation and quenching of triplet excitons by charge carriers at high current densities.

By using a novel *p-i-n* structure in OLEDs, we have successively reduced the operating voltage for both fluorescent [8] and phosphorescent devices [9, 10] in our previous studies. The high conductivity *p-* and *n*-doped layers can enhance the charge injection from the contacts and reduce the ohmic losses in these layers [8, 11-13]. The double emission layer (D-EML) concept for phosphorescent *p-i-n* type OLEDs has been introduced by Zhou et al. in 2002 [14]. Here, we succeed practically to incorporate a D-EML structure in our *p-i-n* phosphorescent OLEDs. The D-EML consists of two layers capable of ambipolar charge transport, one with predominantly hole transporting character, one with predominantly electron transporting character; both are doped with the phosphorescent dye Ir(ppy)$_3$. The D-EML OLEDs show significantly improved efficiency and much lower efficiency loss at high current density compared to conventional single emission layer (S-EML) OLEDs, and higher device stability can also be expected [15,16].

EXPERIMENTAL

It is clear that ultrahigh vacuum environment characteristic of organic thin film deposition processes can provide the necessary material purity and as well as structural and chemical reproducibility necessary in modern, high performance optoelectronic device applications. Vacuum growth of organic materials can generate atomically flat thin films of high purity, facilitating fabrication of complex multi-layer devices with excellent uniformity and sharp interfaces between adjacent layers.

The completed versatile materials growth system in Fig. 2 will integrate the method for physical and vapour phase deposition of hybrid organic/inorganic thin-films with a low-pressure RF/DC sputtering chamber (base pressure ~ 10^{-9} Toor), an evaporative growth chamber (base and operating pressures about 10^{-10} Toor), and a chemical vapour deposition chamber (base pressure ~ 10^{-8} Toor). The completed vacuum system will be capable of depositing molecular organics, polymers, metals, metal oxides, inorganic nanodots, and colloids in a controlled layer-by-layer fashion. An in-situ shadow masking system will enable fabrication of complex patterned structures inside a vacuum environment, while the integrated N$_2$-filled, dry glove box will facilitate handling, measuring, and packaging of organic thin film samples that are susceptible to reactions with atmospheric oxygen and water vapour.

The AFM/STM chambers (base and operating pressures about 10^{-10} Toor) will facilitate in-situ atomic scale microscopy for evaluating morphology and electronic properties of hybrid materials. Samples are analyzed in the analytical and AFM/STM chambers and all connected to the central transfer line with load lock (base and operating pressures about 10^{-7} Toor) and an integrated, nitrogen-filled glove box. All chambers are connected to the central transfer system (base pressure ~ 10^{-9} Toor and operating pressures from 10^{-7} to 10^{-9} Toor) that has linear degrees of freedom. Each chamber is isolated form the others by a gate valve resulting in typical base and operating pressures as indicated above.
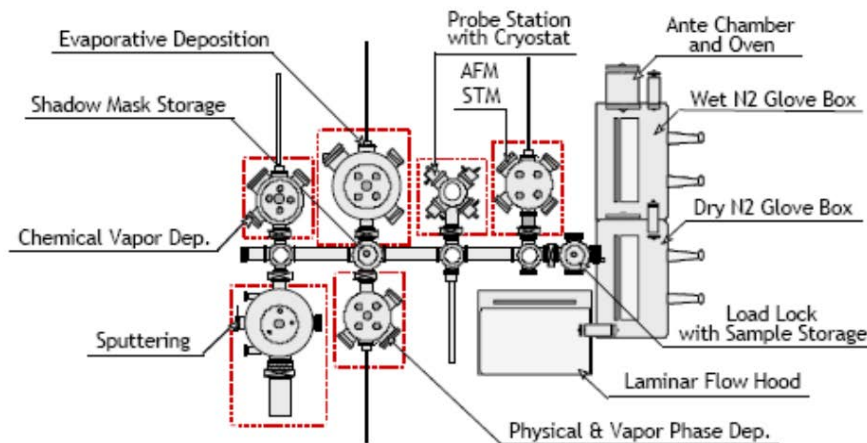

Figure 2   Integrated materials and devices growth system with in-situ shadow masking

Thereby, the OLEDs are prepared by thermal evaporation of different organic layers onto patterned, precleaned and ultraviolet-ozone treated indium tin oxide (ITO) coated glass substrates in an ultrahigh vacuum system at a base pressure of 10^{-8} Torr without breaking vacuum. First, 100-nm-thick N,N,N',N'-tetrakis(4-methoxyphenyl)-benzidine (MeO-TPD) doped with 2 mol.-% of 2,3,5,6-tetrafluoro-7,7,8,8-tetracyanoquino-dimethane (F_4-TCNQ) is deposited as hole injection and transport layer (HTL). This *p*-doped layer has conductivity of approximately 10^{-5} S/cm and forms a quasi-ohmic contact with ITO that ensures easy hole injection via tunneling [17]. Between the *p*-doped HTL and the EML system, an interlayer of 10 nm 2,2',7,7'-tetrakis-(N,N-diphenylamino)-9,9'-spirobifluoren (Spiro-TAD) is deposited as blocking layer (see Fig. 3 below). Next follows the D-EML system comprising a layer of TCTA doped with 8 wt.-% of Ir(ppy)$_3$ and a layer of an electron transporting host like TAZ doped with the same concentration of Ir(ppy)$_3$. Then, another 10-nm-thick interlayer of a material with high electron mobility and appropriate lowest unoccupied molecular orbital (LUMO) level, *e.g.* 4,7-diphenyl-1,10-phenanthroline (BPhen) is deposited to make sure that excitons in the EML are not quenched by the dopants in the electron transport layer (ETL). After that, a 50-nm-thick *n*-doped electron transport layer is obtained by co-evaporation of BPhen with pure Cs from a dispenser source. As the evaporation rate of Cs cannot be measured with a quartz thickness monitor, we prepare a series of doped BPhen layers with different heating power for the Cs dispenser and measure the conductivity in coplanar contact geometry. For the OLEDs, we use a source power where a conductivity of 10^{-5} S/cm is achieved. Finally, a 100-nm-thick cathode layer of aluminum is patterned using a shadow mask, which leads to a device active area of around 3 mm^2. Except of the acceptor dopant F_4-TCNQ, all organic materials have been purified twice by vacuum gradient sublimation.

Moreover, the intrinsic layers consist of the light generating emission layer (EML, around 20 nm in thickness), and of approximately 10 nm thick surrounding blocking layers for electrons (EBL) and holes (HBL) to spatially confine the charges within the EML.

The current–voltage (I–V) and luminance-voltage (L-V) characteristics of the OLEDs are simultaneously measured in-situ under vacuum conditions with a Keithley SMU236, with the luminance obtained by mounting the calibrated silicon photodiode above the OLEDs to detect the light emitted in forward direction through the transparent ITO substrate. The setup is calibrated by comparison with direct luminance measurements using a Minolta CS-100A luminance meter. The quantum efficiency is calculated under the assumptions that the emission pattern is Lambertian and electroluminescence (EL) spectra are angle independent. The EL spectra are recorded by Sentronic PL-USB2000 with an optical fiber attached above the OLEDs in forward direction.

RESULTS AND DISCUSSION

Figure 3 shows the device structure of p-i-n D-EML OLEDs: ITO/MeO-TPD:F_4-TCNQ(100 nm)/Spiro-TAD(10 nm)/TCTA:Ir(ppy)$_3$ (8%, x nm)/ TAZ:Ir(ppy)$_3$ (8%, y nm)/ BPhen(10 nm)/BPhen:Cs(50 nm)/Al, and the energy level diagram of the organic materials used in these devices. The highest occupied molecular orbital (HOMO) and the lowest unoccupied molecular orbital (LUMO) values of the materials used are extracted from the literatures [4, 6, 18].

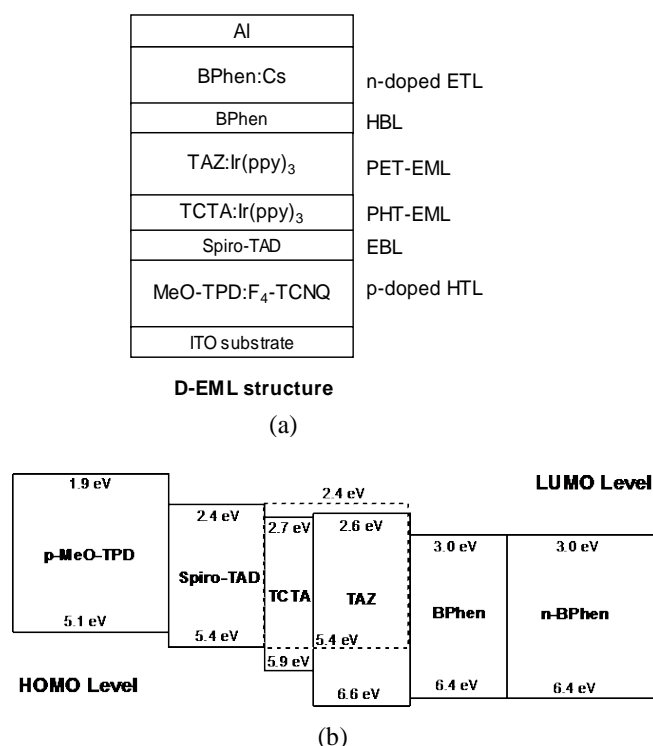|	
Al	
BPhen:Cs	n-doped ETL
BPhen	HBL
TAZ:Ir(ppy)$_3$	PET-EML
TCTA:Ir(ppy)$_3$	PHT-EML
Spiro-TAD	EBL
MeO-TPD:F_4-TCNQ	p-doped HTL
ITO substrate	

D-EML structure

(a)

(b)

Figure 3 (a) Device structure of D-EML *p-i-n* OLEDs and (b) the proposed energy level diagram of the organic materials used in this study.

The Current-Voltage (I–V) and Luminance–Voltage (L–V) characteristics of this D-EML OLED are depicted in Fig. 4. Both I–V and L–V

curves show steep increase after the onset, which is one of the typical characteristics of *p-i-n* OLEDs. The operating voltage for a typical display application brightness of 100 cd/m^2 is 2.95 V, and 1000 cd/m^2 is obtained at only 3.21 V. Moreover, sim4tec at SID had reproduced experimental data for current density and luminance in forward direction of a 5-layer phosphorescent *p-i-n* type OLED using electrical calculation features "SimOLED's". This shows that by carefully determining the material parameters, predictive electrical simulations are possible. As a result of this investigation, the relationship between theoretical and experimental results is proved.
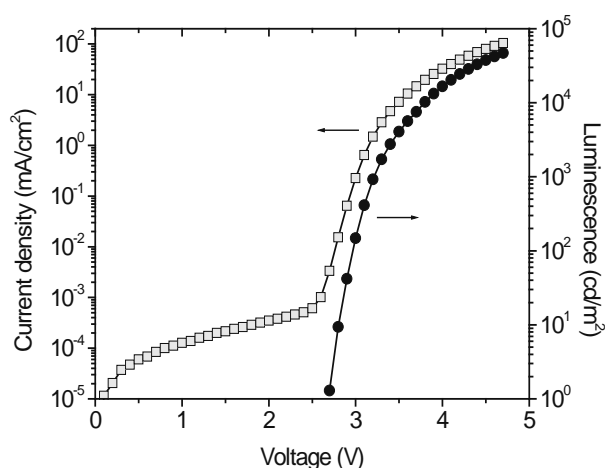

Figure 4   I–V (square, plotted on the left axis) and L–V (circle, plotted on the right axis) characteristics versus voltage for D-EML *p-i-n* OLED with 5 nm PHT-EML and 10 nm PET-EML.

To obtain a deeper insight into the D-EML OLEDs, we have varied the thickness of both emission layers. Figure 5 shows the quantum efficiencies of three D-EML devices with different thickness of emission layers; for comparison, the quantum efficiency of an S-EML device with 20 nm emission layer is depicted as well. For *p-i-n* devices, both holes and electrons can be easily injected from anode and cathode to the organic layers so that operating voltages are low for both S-EML and D-EML devices. Also the S-EML structure using spiro-TAD and BPhen for the blocking layers shows low operating voltage and very high efficiency. However, the plot of quantum efficiency versus current density shown in Fig. 5 reveals significant differences between S-EML and D-EML devices, which can be understood as follows.

For the D-EML device, maximum external quantum efficiency (EQE) of 19.5% at 0.065

mA/cm^2 or at an operating voltage of 2.65 V is obtained with a 5 nm predominantly hole-transporting emission layer (PHT-EML) with TCTA as a host and a 10 nm predominantly electron-transporting emission layer (PET-EML) with TAZ as a host and BPhen for the interlayer at the electron injection side. On the other hand, for the S-EML device, holes tend to accumulate at the interface of TCTA and BPhen due to the large energy barrier, and the recombination occurs in a shallow slab adjacent to this interface. The high density of triplet excitons may lead to enhanced triplet-triplet annihilation [19, 20], while the high density of accumulated holes favours quenching of triplet excitons by charge carriers. The layer sequence of the S-EML device is ITO/MeO-TPD:F$_4$-TCNQ (100 nm)/Spiro-TAD (10 nm)/ TCTA:Ir(ppy)$_3$ (20 nm)/ BPhen (10 nm)/Bphen:Cs (50 nm)/Al. Hence, maximum external quantum efficiency (EQE) of 11.4% at 0.065 mA/cm^2 or at an operating voltage of 2.65 V is obtained for the S-EML device.
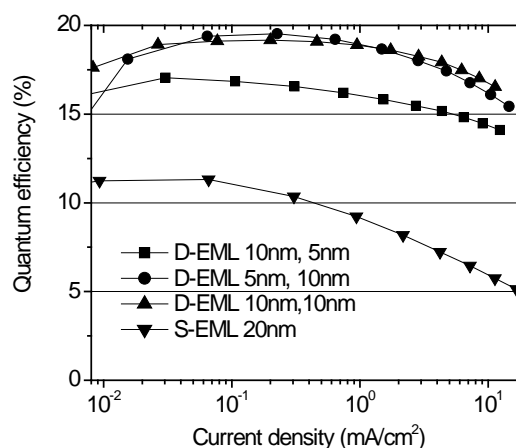

Figure 5   External quantum efficiency versus current density for D-EML devices with various thicknesses of PHT-EML and PET-EML compared with the S-EML device.

Such S-EML devices with TAZ as a hole blocking layer (HBL) show higher efficiency and higher operating voltage compared with the devices using undoped BPhen as HBL. The higher operating voltage can be attributed to the LUMO difference between BPhen and TAZ and lower electron mobility of TAZ. But also here, the efficiency decreases substantially with increasing brightness due to either triple-triplet annihilation or quenching of triplets by accumulated holes at the interface between TCTA and TAZ. In contrast, the D-EML structure can significantly reduce both possible quenching paths by widening the triplet generation zone and avoiding any carrier accumulation at the

interfaces of the EMLs. Moreover, the D-EMLs structures have the potential to optimize the carrier balance at the carrier- recombination interfaces to further improve the device efficiency.

Among the three D-EML devices, the device with thinner doped TAZ emission layer, 5 nm, shows the lowest quantum efficiency. A possible explanation is that holes can penetrate more than 5 nm in PET-EML by hopping through $Ir(ppy)_3$ sites, so some holes reach the interface of TAZ and BPhen and capture electrons to form excitons, which can be quenched by BPhen anion. Between the other two D-EML devices with the same 10 nm think of PET-EML, the device with thinner PHT-EML shows slightly higher efficiency at low current density but faster decay at high current than the device with thicker PHT-EML. As discussed in more detail in our previous work [10] we attribute this to an efficient triplet generation process by holes on $Ir(ppy)_3$ directly capturing electrons without matrix triplets being involved.

The structures discussed above comprise a number of materials with low sublimation temperature or glass transition temperature, namely F_4-TCNQ, MeOTPD, TAZ and undoped BPhen, and are thus not suitable for a real application. In an effort to obtain robust devices, we replaced all these materials by thermally more stable compounds with similar electrical properties and energy levels. The resulting green emitting *p-i-n* type phosphorescent D-EML devices having basically the same layer sequence and working principle are found to have even slightly better performance data as shown in Fig. 6 blow: A power efficiency of 82 lm/W (corresponding to a current efficiency of 66 cd/A) is obtained at 10 cd/m^2, falling to 77 lm/W (corresponding to a current efficiency of 64 cd/A) at 100 cd/m^2, and 64 lm/W (corresponding to a current efficiency of 61 cd/A) at 1000 cd/m^2. The improved power efficiency is due to lower operating voltage, 2.65V at100 cd/m^2 and probably due to the use of a matrix material for the PET-EML with higher electron mobility than TAZ.

Besides the efficiency, high device stability under operation is a further key parameter for organic-based display and lighting applications. The OLED lifetime is usually defined as time until the luminance drops to half of its initial value under constant current operation. Green *p-i-n* type OLED devices operated at room temperature, based on a stacked setup with green phosphorescent emitter materials with 50, 000 hours of operational lifetime at a brightness of 500 cd/m^2 have been realized. Especially the interface between the EML and the HBL is typically a critical point for long term

stability in S-EML OLEDs [21]. Accordingly, the reason for the improved stability is to be found in the fact that the D-EML avoids accumulation of charges at interfaces by its self-balancing character.
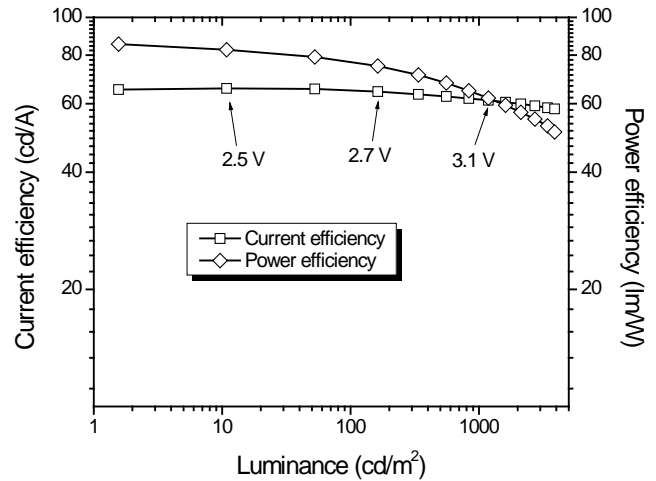

Figure 6   The current efficiencies (square, plotted on the left axis) and power efficiencies (diamond, plotted on the right axis) versus luminance for a D-EML *p-i-n* OLED.

CONCLUSIONS AND RECOMMENDATIONS

In summary, the most efficient OLEDs are grown in high vacuum systems using thermal evaporation sources. New roll-to-roll manufacturing techniques offer the best opportunity for mass production of low-cost OLEDs, and these processes may eventually make the cost of producing OLEDs competitive. Thereby, we have demonstrated high-efficiency and low-voltage *p-i-n* phosphorescent OLED by doping $Ir(ppy)_3$ into both hole transport host and electron transport host. A luminance of 100 cd/m^2 is obtained at 2.65 V with a power efficiency of 77 lm/W, and even at 1000 cd/m^2 the power efficiency is still above 60 lm/W. The color coordinates for this device in a standard bottom-emission structure are CIE chromaticity coordinates (x = 0.26, y = 0.68). Our data suggest a promising approach for low-power display and lighting device applications. To date, among the most important challenges are achieving high material purity, low-cost, high brightness, and long operational lifetime of OLEDs for practical applications.

ACKNOWLEDGEMENTS

REFERENCES

[1] Baldo, M. A., O'Brien, D. F., You, Y., Shoustikov, A., Sibley, S., Thompson, M. E., and Forrest, S. R., Highly efficient phosphorescent emission from organic electroluminescent devices, *Nature* Vol. 395, 1998, PP. 151-154.

[2] Baldo, M.A., Lamansky, S., Burrows, P.E., Thompson, M.E., and Forrest, S.R., Very *High-Efficiency Green Organic Light-Emitting Devices based on Electro-phosphorescence*, Applied Physics Letters Vol. 75, 1999, pp. 4-6.

[3] Thompson, M.E., Burrows, P.E., and Forrest, S.R., *Electrophosphorescence in Organic Light Emitting Diodes*, Current Opinion in Solid State & Materials Scienc*e* Vol.4, 1999, pp. 369-372.

[4] Adachi, C., Baldo, M.A., Forrest, S.R., Lamansky, S., Thompson, M.E., and Kwong, R.C., *High-efficiency Red Electro-phosphorescence Devices*, Applied Physics Letters Vol. 78, 2001, pp. 1622-1624.

[5] Adachi, C., Baldo, M. A., Thompson, M. E., and Forrest, S. R., "*Nearly 100% Internal Phosphorescence Efficiency in an Organic Light-Emitting Devic*e", Journal of Applied Physics Vol. 90, 2001, pp. 5048-51.

[6] Ikai, M., Tokito, S., Sakamoto, Y., Suzuki, T., and Taga, Y., *Highly Efficient Phosphorescence from Organic Light-Emitting Devices with an Exciton-Block Layer*, Applied Physics Letters Vol. 79, 2001, PP. 156-158.

[7] Adachi, C., Baldo, M. A., Forrest, S. R., and Thompson, M. E., *High-Efficiency Organic Electrophosphorescent Devices with tris(2-phenylpyridine)iridium doped into electron-transporting materials*, Applied Physics Letters Vol. 77, 2000, pp. 904-906.

[8] Huang, J., Pfeiffer, M., Werner, A., Blochwitz, J., Liu, S., and Leo, K., *Low-Voltage Organic Electroluminescent Devices using Pin Structures*, Applied Physics Letters Vol. 80, 2002, pp. 139-141.

[9] Pfeiffer, M., Forrest, S. R., Leo, K., and Thompson, M. E., *Electrophosphorescent p-i-n Organic Light Emitting Devices for Very High Efficiency Flat Panel Displays*, Advanced Materials, Vol. 14, 2002, pp. 1633-1636.

[10] He, G., Schneider, O., Qin, D., Zhou, X., Pfeiffer, M., and Leo, K., *Very High-Efficiency and Low Voltage Phosphorescent Organic Light-Emitting Diodes based on a p-i-n Junction*, Journal of Applied Physics Vol. 95, 2004, pp. 5773.

[11] Yamamori, A., Adachi, C., Koyama, T., and Taniguchi, Y., *Doped Organic Light Emitting Diodes having a 650-nm-thick Hole Transport Layer*, Applied Physics Letters Vol. 72, 1998, pp. 2147-2149.

[12] Blochwitz, J., Pfeiffer, M., Fritz, T., and Leo, K., *Low Voltage Organic Light Emitting Diodes Featuring Doped Phthalocyanine as Hole Transport Material*, Applied Physics Letters Vol. 73, 1998, pp. 729-731.

[13] Zhou, X., Pfeiffer, M., Blochwitz, J., Werner, A., Nollau, A., Fritz, T., and Leo, K., *Very Low Operating Voltage Organic Light-Emitting Diodes using a p-doped Amorphous Hole Injection Layer*, Applied Physics Letters, Vol. 78, 2001, pp. 410-412.

[14] Zhou, X., Qin, D.S., Pfeiffer, M., Blochwitz-Nimoth, J., Werner, A., Drechsel, J., Maennig, B., Leo, K., Bold, M., Erk, P., and Hartmann, H., *High-Efficiency Electro-phosphorescent Organic Light-Emitting Diodes with Double Light-Emitting Layers*, Applied Physics Letters Vol. 81, 2002, pp. 4070-4072.

[15] Popovic, Z.D., Xie, S., Hu, N., Hor, A., Fork, D., Anderson, G., and Tripp, C., *Life Extension of Organic LED's by Doping of a Hole Transport Layer*, Thin Solid Films Vol. 363, 2000, pp. 6-8.

[16] Blochwitz, J., Fritz, T., Pfeiffer, M., Leo, K., Alloway, D.M., Lee, P.A. and Armstrong, N.R., *Interface Electronic Structure of Organic Semiconductors with Controlled Doping Levels*, Organic Electronics Vol. 2, 2001, pp. 97-104.

[17] Wu, C.C., Lin, Y.T., Wong, K.T., Chen, R.T., and Chien, Y.Y., *Efficient Organic Blue-Light-Emitting Devices with Double Confinement on Terfluorenes with Ambipolar Carrier Transport Properties*, Advanced Materials Vol. 16, 2004, pp. 61-65.

[18] Baldo, M.A. and Forrest, S.R., *Transient Analysis of Organic Electro-phosphorescence. II.* Transient Analysis of Triplet-Triplet Annihilation, Physical Review B: Condensed Matter Vol. 62, 2000, pp. 10967-10977.

[19] Adachi, C., Kwong, R., and Forrest, S.R., *Efficient Electrophosphorescence using a Doped Ambipolar Conductive Molecular Organic Thin Film*, Organic Electronics Vol. 2, 2001, pp. 37-43.

[20] Kwong, R.C., Nugent, M.R., Michalski, L., Ngo, T., Rajan, K., Tung, Y.-J., Weaver, M.S., Zhou, T.X., Hack, M., Thompson, M.E., Forrest, S.R., and Brown, J.J., *High Operational Stability of electro-phosphorescent Devices*, Applied Physics Letters Vol. 81, 2002, pp. 162-164.

[21] Tang, C.W., *Two-Layer Organic Photo-voltaic Cells,* Applies Physics Letters Vol. 48, 1986, pp. 183.